Structure and dynamics of intercalation complexes of anthracyclines with d(CGATCG)$_2$ and d(CGTACG)$_2$. 2D-^{1}H and ^{31}P NMR investigations

Stefania Mazzini, Rosanna Mondelli * and Enzio Ragg

Dipartimento di Scienze Molecolari Agroalimentari, Sezione di Chimica, Universitá degli Studi di Milano, Via Celoria 2, 20133 Milano, Italy

The interaction of (2*S*)-2-methoxymorpholinodoxorubicin 4 and morpholinodoxorubicin 5 with the hexanucleotides d(CGATCG)$_2$ and d(CGTACG)$_2$ has been studied by a combined use of 2D-^{1}H and ^{31}P NMR techniques and molecular dynamics (MD) calculations, in comparison with doxorubicin 1, daunorubicin 2 and idarubicin 3. Both ^{1}H and ^{31}P chemical shifts of imino protons and phosphates respectively have been shown to be a sensitive probe for the intercalation sites (two anthracycline molecules at the CpG sites). A relevant number of NOE interactions allowed the structure of the complexes in solution to be derived through restrained MD calculations, which were compared with those obtained by X-ray analysis. In all the complexes the aglycone was shown to be located in the middle of the double helix, orthogonally oriented with respect to the base pairs, with ring D extending out of the helix on the major groove and ring A, with $^9H_8$ conformation, between guanines G$_2$ and G$_{12}$. The daunosamine and morpholino moieties lie in the center of the minor groove, with slightly different positions than in the X-ray structures. In all the complexes the daunosamine ring is located at the A$_3$ (T$_3$) level, while the morpholino ring displays NOE interactions with the fourth unit T$_4$ (A$_4$). The deformations of the double helix are revealed by an increased distance between protons of the C$_5$ and G$_6$ units and by conformational changes at the level of the *α*, *ζ*, *ε* and *δ* angles of the phosphoribose backbone. The variation of the ^{31}P chemical shifts is interpreted in terms of conformational equilibria leading to different populations of conformers. This is clearly shown from the values of the *α* and *ζ* torsion angles, monitored during the MD, which indicate a relevant population of *trans* forms for *ζ* and also for *α* angles of C$_5$pG$_6$ and G$_2$pT$_3$ (G$_2$pA$_3$) units, while the other phosphates exist entirely in the *α*, *ζ*, *gauche*,*gauche* conformation. The dissociation rate constants were measured by 2D ^{31}P NOESY-exchange experiments for 1 and 4. The decrease of k_{off} for 4, corresponding to a ten-fold increase of the residence time of the drug in the intercalation sites, is in line with the higher activity found for methoxymorpholinodoxorubicin 4.

Introduction

Doxorubicin (adriamycin) **1** and daunorubicin (daunomycin) **2** are still currently used in cancer chemotherapy, although their clinical use is limited by unfavourable side effects such as cardiotoxicity, myelosuppression and development of drug resistance.[1] Among the hundreds of natural, synthetic and semisynthetic analogues, the morpholinyl derivatives **4** and **5** of doxorubicin[2] have shown an outstandingly potent antitumor activity in conjunction with less side effects, in particular the lack of cardiotoxicity at therapeutically effective doses.[3] The morpholinyl analogues appear to have a mechanism of action that differs from that of the parent anthracyclines. In spite of many years of study, the mechanism by which all these molecules mediate their relatively selective antitumor effect is not yet clear, nor the way by which they may damage DNA.[4] Some morpholinyl derivatives seem to be able to bind covalently to DNA and also to induce DNA cross-linking.[3a,5,6] This proposed binding, proved for anthracyclines with a cyanomorpholinyl group, is still questioned for other morpholinyl derivatives.[6] The binding to DNA seems to be critical for antitumor activity; this justifies the great effort that has been devoted to finding the nucleotide sequence preference in the anthracycline–DNA interactions. Theoretical[7] and experimental[8–11] results have shown that the preferred triplet binding site is 5′-CGA or 5′-CGT. The three-dimensional structure of DNA–anthracycline complexes has usually been obtained by X-ray crystallography, and NMR studies[12] have been found to be in substantial agreement with the structures in solid phase.[10,11] The complex of DNA with menogaril, an anthracycline of a different family, has recently been studied in solution by NMR.[13]

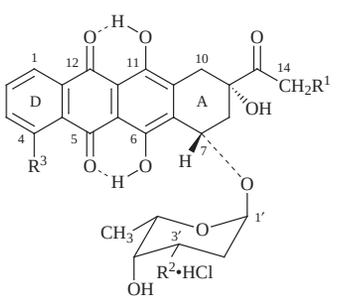

1 R^1 = OH, R^2 = NH$_2$, R^3 = OCH$_3$
2 R^1 = H, R^2 = NH$_2$, R^3 = OCH$_3$
3 R^1 = H, R^2 = NH$_2$, R^3 = H

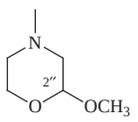

4 R^1 = OH, R^2 = R^3 = OCH$_3$

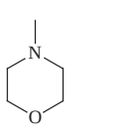

5 R^1 = OH, R^2 = R^3 = OCH$_3$

In our preceding studies on the interaction between d(CGTACG)$_2$ and anthracyclines of dauno/doxo family[9] we have used ^{31}P NMR spectroscopy; we have identified the intercalation site and obtained thermodynamic and kinetic parameters of the process. The binding constants have been found to

depend on the ionic strength and the self-association, so much so that their measurement by NMR to study anthracycline–DNA interactions was not recommended. In contrast, the dissociation rate constants (k_{off}) of the slow step of the intercalation process can be measured with high accuracy directly by NMR NOE-exchange experiments and were found not to depend upon ionic strength and self-association phenomena. The kinetic constants are an expression of the average residence time of the drug in the intercalation sites ($1/k_{off}$), a parameter which appears to be related to the cytotoxic activity: in the case of morpholinyl derivatives, the residence time between the CG base pairs has been found to be longer than for the parent compound, in line with the increased activity. These results suggested the extension of this study to other DNA sequences. We used the hexanucleotide $d(CGATCG)_2$ and the active new generation morpholinyl analogues **4** and **5**. We performed ^{31}P and ^{1}H NOE experiments on the complexes obtained with both the oligonucleotides $d(CGTACG)_2$ and $d(CGATCG)_2$, in order to find whether the binding is affected by the change in the triplet, CGT *vs*. CGA, to detect the contacts between anthracycline and the DNA fragment, and to establish whether a covalent binding occurs in the case of methoxymorpholinodoxorubicin **4**.

Experimental

The self-complementary oligodeoxynucleotides $d(CGTACG)_2$ and $d(CGATCG)_2$ sodium salts, synthesized in the solid phase using a phosphotriester method and purified by HPLC, as well as doxorubicin **1**, daunorubicin **2**, idarubicin **3**, (2*S*)-2-methoxymorpholino- **4** and morpholinodoxorubicin **5**, were a kind gift from Pharmacia & Upjohn. The hexanucleotides were dissolved in 0.6 ml of D_2O with low paramagnetic impurities or H_2O–D_2O (9 : 1), HPLC grade, in the presence of 0.1 mol dm^{-3} or 1 mol dm^{-3} NaCl and 10 mmol dm^{-3} phosphate buffer (pH 6.7) (uncorrected pH meter) and 1 mmol dm^{-3} EDTA. The concentration (1.7 mmol dm^{-3}) of the oligonucleotides was determined by means of the UV absorbance $\varepsilon = 53\,630$ dm^3 mol^{-1} cm^{-1} for the single strand. The UV measurements were made on a JASCO 7800 instrument. The NMR titration experiments were performed by adding increasing amounts of a concentrated solution (20 mmol dm^{-3}) of the drug to a solution of the oligonucleotide. The formation of the complex was monitored by recording ^{31}P and ^{1}H NMR spectra.

NMR Experiments

The ^{1}H NMR spectra were recorded on Bruker AMX 600 and Varian XL 300 spectrometers, operating at a frequency of 600.13 and 300.1 MHz, respectively for the ^{1}H nucleus. ^{31}P NMR spectra were recorded with the Bruker AMX 600 spectrometer, operating at a frequency of 242.94 MHz for ^{31}P nucleus. ^{1}H and ^{31}P chemical shifts were measured in δ (ppm) and referenced respectively to 3-(trimethylsilyl)propanesulfonic acid sodium salt and 1% H_3PO_4 (external reference). The two-dimensional spectra were acquired in the phase sensitive TPPI mode. DQF-COSY spectra were performed on the oligonucleotides and on the complexes in D_2O buffer solution. TOCSY spectra[14a] were recorded with the use of the MLEV-17[14b] spin-lock pulse (field strength 7576 Hz, 60 ms total duration). ^{1}H NOESY spectra were acquired at mixing times of 100, 300 and 500 ms at 25 and 45 °C. Water suppression was achieved with pre-saturation with the carrier frequency placed on the H_2O resonance. When exchangeable protons had to be observed, the suppression of the H_2O signal was obtained by the '1-1 echo' pulse sequence,[14c] using a 0.5 ms homospoil pulse and a 50 μs delay, in order to obtain the maximum excitation centered on the imino proton resonance region. An average number of 512 to 1024 × 2k FIDs were collected with 1.5 s recycling delay, 7000 Hz spectral width, 80 scans, total acquisition time of 16 h. FIDs were processed with zero filling to 1k × 2k real data points and weighted with a 90° shifted sine-bell squared function. A baseline correction was then applied using a third-order polynomial. The dissociation rate constants were obtained by 2D ^{31}P NOESY experiments, performed with [drug]/[DNA] ratios equal to 0.5 and 1.0, at different mixing times ranging from 20 to 800 ms. 2D ^{31}P NOESY experiments were acquired (256 × 1k FIDs, 196 scans) and transformed by standard methods. ^{13}C NMR spectra of the anthracycline drugs were obtained by one-bond correlation spectroscopy in 'reverse' detection mode, using HMQC[14d] experiments with water pre-saturation.

Computer-aided molecular modelling

Molecular models were built using a Silicon Graphics 4D35GT workstation running the Insight II & Discover software. The anthracyclines and the oligonucleotides in the canonical B-DNA form were generated using standard bond lengths and angles. The drug–DNA complexes were then constructed by interactive graphics, qualitatively following the NOE data. NOE constraints were then applied using a harmonic potential, with a pseudo-energy constant set to zero whenever the error function was between 2 and 4 Å and set to 41.8 kJ mol^{-1} $Å^{-2}$ whenever the error function was outside the same limits. The models were energy minimized and a subsequent restrained molecular dynamics calculation was performed for 92 ps at 600 K temperature, sampling the trajectory every 2 ps. A final structure was obtained by energy minimization of the last twenty structures. Torsion angles and interatomic distances were obtained from the final geometry. The probable errors were estimated on the basis of another set of twelve energy minimized structures, generated by a 24 ps MD run at 400 K. The AMBER[15] forcefield was used for all the simulations, without explicit inclusion of solvent molecules, setting a distance-dependent relative permittivity $\varepsilon_r = 4.0$ and scaling the 1–4 nonbond interactions by a factor of 0.5. For the anthracycline atoms, the potentials were set by similarity with the DNA aromatic and sugar atoms.

Results and discussion

^{31}P NMR assignments and measurements of the dissociation rate constants for the complexes with $d(CGATCG)_2$ and $d(CGTACG)_2$

We followed the formation of the reversible anthracycline–oligonucleotide complexes by recording ^{31}P NMR spectra at different ratios R = [drug]/[DNA] and at different temperatures. At room temperature, the intercalation process of daunorubicin **2** and its derivative, idarubicin **3**, lies in an intermediate chemical exchange regime on the NMR time scale, with a broadening of all resonances, whereas for doxorubicin **1** and its morpholinyl derivatives **4** and **5** the process is slow.[9] The DNA fragments $d(CGATCG)_2$ and $d(CGTACG)_2$, henceforth referred to as 'AT' and 'TA' respectively, exist as double helices[16] in solutions of moderate ionic strength. Each NMR signal derives from the resonance of two distinct nuclei because of the inherent two-fold symmetry of the double helix. The addition of doxorubicin **1** or methoxymorpholinodoxorubicin **4** to a solution of the oligomer $d(CGATCG)_2$ induces the appearance of three new peaks at low field in the ^{31}P NMR spectrum, as shown in Fig.1. The assignment of the phosphate groups was performed by means of 2D ^{31}P NOESY-exchange experiments at low [drug]/[DNA] ratios, as the assignments for the free nucleotides are known.[9,16] An example of such a spectrum is reported in Fig. 2, which shows the correlations between signals belonging to the phosphate groups of bound species (at low field) in chemical exchange with those of the same groups in the free state. The strongest low field shift ($\Delta\delta$ 1.57 ppm for **1** and $\Delta\delta$ 1.20 ppm for **4**, see Table 1) was observed for phosphate C_5pG_6, which was thus identified as the intercalation site. The other two downfield signals were assigned to G_2pA_3 and C_1pG_2

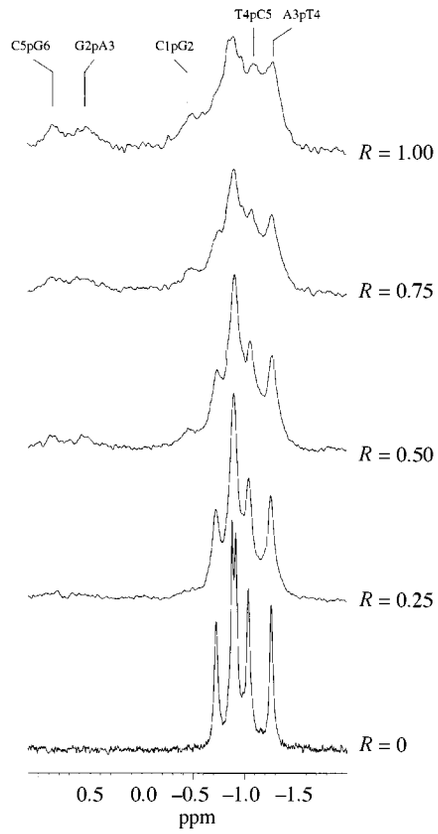

Fig. 1 ^{1}H-decoupled ^{31}P NMR spectra in 10 mmol dm^{-3} phosphate buffer (pH 6.7), 1 mol dm^{-3} NaCl, 25 °C, of d(CGATCG)$_2$ in the presence of doxorubicin **1** at different ratios R = [**1**]/[DNA]

($\Delta\delta$ 1.05 ppm and $\Delta\delta$ 0.59 ppm, respectively in the case of 'AT'–**4**). The internal phosphates A_3pT_4 and T_4pC_5 are not well defined in the spectrum of Fig. 2, because they are partially overlapped with the resonances of the free species. Experiments in different conditions are not better resolved, but indicate that these phosphates present a small shift variation. A $\Delta\delta = -0.1$ ppm could be measured for A_3pT_4 in 'AT'–**4**, whereas the values for the other phosphates were estimated to be less than 0.2 ppm.

The intensity of the C_5pG_6 signal in the bound state, reported as a function of the ratio R = [drug]/[DNA], gave a stoichiometry of two drug molecules per duplex. The second molecule of drug intercalates at the symmetrically located C_5pG_6 site on the opposite strand, thus restoring the C_2 symmetry (this is more clearly visible in ^{1}H NMR spectra). An inspection of Table 1 shows that the chemical shift variation in the complexes with 'AT' are similar to those observed for the complexes with 'TA' nucleotide,[9b] with the exception of G_2pT_3 and G_2pA_3. The main factor which determines ^{31}P chemical shift variations in nucleotides is the conformation of the phosphodiester groups at the level of the P–O(5′) and O(3′)–P bonds, *i.e.* the values of the torsion angles α = O(3′)–P–O(5′)–C(5′) and ζ = C(3′)–O(3′)–P–O(5′). For a nucleotide in a B-DNA type conformation the phosphate groups are normally found in the *gauche*,*gauche* (*g*,*g*) conformation, with α and ζ angles of −60 and −90° respectively, whereas the *gauche*,*trans* conformation (α = −60, ζ = 180°) is generally associated with a deshielding of *ca.* 1.5 ppm.[17] The relevant low field shift of phosphates C_5pG_6, G_2pT_3 and G_2pA_3, observed for the 'TA' and 'AT' complexes, indicates a conformational change, which should result in a predominant arrangement in *g*,*t* conformations (see later). Similar deformations do not occur in the complementary strand; the small low field shift observed in both complexes for the terminal phosphate C_1pG_2, whose bases are hydrogen bonded to C_5pG_6, is at first sight unexpected, but originates from the asymmetric shape of the intercalating molecules.

Table 1 ^{31}P chemical shift assignments (δ) for d(CGATCG)$_2$ and d(CGTACG)$_2$ in the free duplex and in the complex with anthracyclines **1** and **4**[a]

Phosphate group	Free duplex d(CGATCG)$_2$	Complex with anthracyclines		$\Delta\delta$ = $\delta_{bound} - \delta_{free}$	
		1	**4**	**1**	**4**
C_1pG_2	−0.91	−0.48	−0.32	+0.43	+0.59
G_2pA_3	−0.86	+0.67	+0.19	+1.53	+1.05
A_3pT_4	−1.26	−1.28[b]	−1.36	≤0.2[c]	−0.1
T_4pC_5	−1.06	−1.12[b]	−1.11	≤0.2[c]	≤0.2[c]
C_5pG_6	−0.73	+0.84	+0.52	+1.57	+1.25

Phosphate group	Free duplex d(CGTACG)$_2$	Complex with anthracyclines		$\Delta\delta$ = $\delta_{bound} - \delta_{free}$	
		1	**4**	**1**	**4**
C_1pG_2	−1.03	−0.58	−0.56	+0.45	+0..47
G_2pT_3	−1.40	−0.56	−0.50	+0.84	+0.90
T_3pA_4	−1.12	−1.26	−1.45	−0.14	−0.33
A_4pC_5	−1.20	−1.34	−1.46	−0.14	−0.26
C_5pG_6	−0.90	+0.63	+0.22	+1.53	+1.12

[a] Spectra acquired at 242.94 MHz, 25 °C, 10 mmol dm^{-3} phosphate buffer and 1 mol dm^{-3} NaCl. The values for d(CGTACG)$_2$ are taken from ref. 9*b*. Accuracy within 0.05 ppm unless otherwise specified. [b] Accuracy of 0.1 ppm. [c] Estimated value.

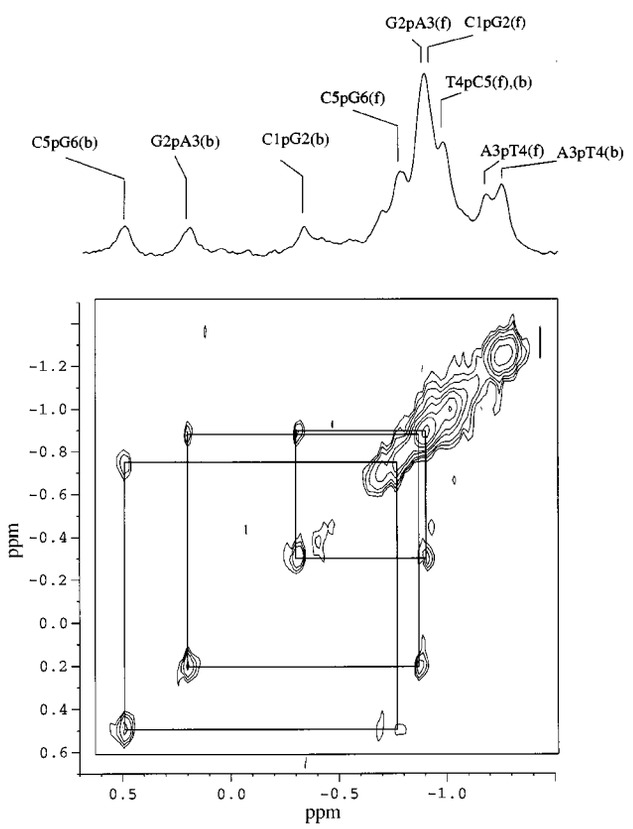

Fig. 2 An example of a ^{31}P NOESY exchange spectrum for the 'AT'–**4** complex (R = [**4**]/[DNA] = 0.5, t_{mix} 150 ms. The other experimental conditions are as in Fig.1).

The kinetic aspects of the interaction between doxorubicin **1** and methoxymorpholinodoxorubicin **4** with d(CGATCG)$_2$ were studied by means of 2D ^{31}P NOESY-exchange experiments, following the procedure previously set[9b] to study anthracycline–'TA' complexes. The average residence time of the drug in the intercalation sites is an important factor to be considered in the study of the antimitotic activity of the anthracyclines. This parameter is related to the inverse of the dissociation rate

Table 2 Values of the dissociation rate constants (k_{off}/s^{-1}), average life time (k_{off}^{-1}/s) and activation energies $\Delta G^{\ddagger}$ at 25 °C, for the complexes of d(CGATCG)$_2$ with anthracyclines **1** and **4**

Compound	k_{off}/s^{-1}	k_{off}^{-1}/s	$\Delta G^{\ddagger}$/kJ mol^{-1}
Doxorubicin **1**	23.0 ± 4.0	0.043 ± 0.01	65.21 ± 1.74
Methoxy-morpholinodoxo-rubicin **4**	2.4 ± 1.15	0.41 ± 0.19	71.15 ± 1.30

constant and can be directly determined with high accuracy by quantification of ^{31}P signal intensities in NOESY experiments performed at different mixing times. It is relevant that this rate constant was found[9b] to be independent from ionic strength and self-association. The dissociation rate constants k_{off} and the activation energies $\Delta G^{\ddagger}$, calculated by solving the Eyring equation, are reported in Table 2. The decrease of k_{off} for methoxymorpholinodoxorubicin **4**, with respect to the parent compound **1**, corresponds to a ten-fold increase of the residence time of the drug in the intercalation sites and must be related to the higher activity found[3b] *in vivo* and *in vitro* for **4** *vs.* **1**. This result is in line with the data obtained[9b] for 'TA' complexes and shows that in this case the difference in the nucleotide sequence CGT *vs.* CGA does not affect this parameter. As a consequence, it appears that structural modifications at the level of ring A and of the aminosugar in the anthracycline molecule are very important, and that the methoxymorpholino moiety plays a significant role in the stability of the complexes. In particular the presence of the methoxy group is important, as shown in previous studies[9b] on the 'TA' complexes with morpholino- and 2′-methoxymorpholinodoxorubicin **4** and **5**. The increase in k_{off} from 2.2 s^{-1} for **4** to 8.2 s^{-1} for **5** indicates a direct involvement of the methoxy group. This is in line with the higher cytotoxicity of **4** with respect to **5**.[3b] However the reasons why the residence time of **4** in the complex is longer than for **5** are not clear. One explanation may be that the methoxy oxygen atom is involved in hydrogen bonding with the oligonucleotide unit. As the A_4 residue in front of the morpholino ring (see Conclusions section) does not contain free donor groups, the hydrogen bonds should be mediated by the water molecules.

Assignment of oligonucleotide and drug protons in the complexes

As soon as a non-symmetric drug binds to the double helix, the C_2 symmetry axis is destroyed and the two strands of the oligonucleotide are no longer equivalent. As a consequence, the protons belonging to the two strands, which are symmetrically related in the free oligonucleotide, are also non-equivalent and give rise to separate signals, which show in NOESY and TOCSY spectra exchange correlations. The chemical exchange between the two strands is due to a 'flip-flop' mechanism, similar to that found for minor groove binders;[4a] in other words the anthraquinone ring system of the drug intercalates alternately between the two CG sites (C_5pG_6 and $C_{11}pG_{12}$), thus inducing the exchange of the chemical environments of the two strands. For instance, for the complex with d(CGATCG)$_2$ the adenine 8-H on one strand (A_3) exchanges with the same proton on the other strand (A_9). When R = [drug]/[DNA] is equal to 1, the free nucleotide is still present in solution and shows additional resonances in chemical exchange with the corresponding signals of the bound oligonucleotide. Increasing R from 1 to 4, the signals of the free oligonucleotide disappear and the resonances of the bound residues give rise to a simple pattern, as the C_2 symmetry is restored by the formation of a symmetrical complex involving two molecules of anthracycline per self-complementary oligomer.

The ^{1}H NMR spectra of the complexes between 'TA' and doxorubicin **1**, daunorubicin **2** and idarubicin **3** were recorded at 45 °C and 300 MHz. At room temperature, the addition of increasing amounts of drug to the oligonucleotide solution causes a dramatic and generalized line broadening of DNA signals; this effect is even enhanced at 600 MHz. The increase in line-width with magnetic field due to the increased relaxation times T_2 of nuclei, which is actually a function of the magnetic field, indicates the formation of high molecular weight species. The anthracyclines, when present in solution in excess to the oligomer, tend to aggregate and to form non-specific complexes by outside-binding to the double helix. This is due to the binding of a negatively charged polyion, like DNA, with a positively charged polyion, like the one formed by anthracycline self-association.[4a,8c] At 45 °C and 300 MHz, in the case of complexes with anthracyclines **1**–**3**, the exchange process is fast with respect to the NMR time scale, whereas at room temperature an intermediate chemical exchange regime can occur. At 45 °C the molecular tumbling of the aggregated species is faster, so that the ^{1}H resonances are sufficiently narrow to be followed individually through the titration. In contrast, both the complexes of morpholinyl analogues **4** and **5** with 'TA' and 'AT' nucleotides gave spectra at 600 MHz and room temperature with a fairly good resolution, in spite of the spectral complexity, due to the slow exchange regime.

The sequential assignment of the nucleotide units in the complexes was performed by following standard rules[18] for a B-type double helix, *i.e.* by using the inter-residue NOE interactions between the aromatic protons of the bases and the ribose 1′-H and 2′,2″-H of the 5′-neighbour unit (Fig. 3). The starting point for the sequential assignments was the identification of cytidine protons 5-H and 6-H due to their characteristic three-bond coupling constants, through the intense TOCSY and COSY cross peaks, and the identification of thymine 6-H protons through the weak TOCSY connectivity due to the four-bond coupling with their methyl groups. 6-H and 5-H protons of the internal cytidines $C_{5,11}$ † were detected at higher fields than those of the terminal cytidines $C_{1,7}$, as occurs in the free oligonucleotide. The ribose 1′, 2′ and 2″-H of $C_{1,7}$ were thus assigned by the interaction with 5,6-H of the same residue; this allowed in turn the assignment of 8-H of $G_{2,8}$. The guanine 8-H protons interact with the thymine 6-H and with the adenine 8-H of 'TA' and 'AT' complex respectively. Thus 6-H and 8-H protons of T_3 and A_3 units could be attributed in the two oligonucleotide sequences. In this way, by using the above mentioned strategy, it was possible to move along the strand from the 5′-end to the 3′-end and to establish the sequential assignment for aromatic and ribose protons. The sequence breaks off at the level of the C_5–G_6 units, which are thus more displaced and can adjust the intercalating molecule. The chemical shift values of aromatic and ribose protons (1′-H and 2′,2″-H) for both nucleotides, with and without intercalating drugs, are reported in Table 3. The remaining ribose protons 3′,4′,5′,5″-H were all assigned but are not reported in Table 3, as they did not show significant NOE interactions, except for 4′-H of T_3 and 4′,5′,5″-H of A_4 in the 'TA' complex and for 4′-H of G_{12} in both complexes (see later).

The imino protons of the bases resonate in a relatively free region of the spectrum, between 12 and 14 ppm, so that the assignment was not difficult (Table 3). In the case of a hexamer with C_2 symmetry a maximum of three signals can be found, but at room temperature only two resonances were observed even without pre-saturation of the HOD resonance. The missing signal relates to the imino protons of the terminal C_1:G_{12} and G_6:C_7 base pairs, in rapid exchange with the solvent, owing to the 'fraying' process. The addition of increasing amounts of drug to both oligonucleotides results in a number of new resonances, which do not shift but increase in intensity as R = [drug]/[DNA] is increased. When R = 1 the lack of the C_2 symmetry

† One strand is numbered from C_1 to G_6 and the complementary strand from C_7 to G_{12}.

Table 3 ^{1}H Chemical shift assignments (δ) for the complexes of d(CGATCG)$_2$ and d(CGTACG)$_2$ with anthracyclines **1**, **2**, **3**, **4** and **5**

DNA protons[a]	'AT'[c]	'AT' + **4**[c]	'TA'[c]	'TA' + **4**[c]	'TA' + **5**[c]	'TA'[d]	'TA' + **1**[d]	'TA' + **2**[d]	'TA' + **3**[d]
6-H C_1[b]	7.61	7.60	7.55	7.70	7.70	7.50	7.50	7.52	7.55
8-H G_2	7.99	8.10	7.95	8.10	8.20	7.91	7.91	7.92	8.00
8-H A_3/6-H T_3[e]	8.32	8.19	7.20	7.30	7.31	7.20	7.33	7.20	7.25
2-H A_3/A_4[e]	7.95	8.00	7.56	7.44	7.47	7.52	7.52	7.52	7.25
6-H T_4/8-H A_4[e]	7.23	7.02	8.31	8.21	8.21	8.21	8.10	8.17	8.15
6-H C_5	7.50	7.20	7.25	7.20	7.30	7.35	7.26	7.30	7.30
8-H G_6	7.96	7.92	7.81	7.95	7.90	7.80	7.85	7.85	7.85
5-H C_1	5.89	5.40	5.75	5.60	5.70	5.91	5.41	5.74	5.60
5-H C_5	5.71	5.31	5.33	4.75	5.31	5.50	5.41	5.28	5.00
5-Me T_3/T_4[e]	1.20	1.00	1.50	1.30	1.45	1.42	1.20	1.42	1.38
1′-H C_1	5.76	5.80	5.62	5.97	5.74	5.91	5.80	5.85	5.80
1′-H G_2	5.60	5.30	5.90	5.57	5.61	5.95	5.51	5.85	5.80
1′-H A_3/T_3[e]	6.34	6.00	5.50	5.50	5.65	5.91	5.55	5.76	5.70
1′-H T_4/A_4[e]	5.99	6.00	6.18	6.20	6.18	6.20	6.00	6.13	6.10
1′-H C_5	5.90	6.00	5.50	5.58	5.60	5.81	5.60	5.74	5.70
1′-H G_6	6.18	6.10	6.00	6.18	6.18	6.07	6.05	5.74	6.05
2′,2″-H C_1	2.41, 1.88	2.30, 1.80	2.20, 2.00	2.37, 1.95	2.32, 1.90	2.61, 2.61	2.11, 1.81	2.30, 1.80	2.50, 2.10
2′,2″-H G_2	2.86, 2.76	2.75, 2.65	2.73, 2.73	2.80, 2.55	2.81, 2.70	2.61, 2.15	2.50, 2.50	2.61, 2.61	2.65, 2.65
2′,2″-H A_3/T_3[e]	2.30, 2.73	2.83, 2.60	2.43, 2.21	2.15, 1.85	2.35, 1.95	2.31, 1.85	2.20, 1.85	2.10, 1.80	2.25, 1.95
2′,2″-H T_4/A_4[e]	2.47, 2.04	2.50, 2.21	2.80, 2.73	2.73, 2.56	2.90, 2.70	2.70, 2.61	2.65, 2.55	2.89, 2.67	2.75, 2.60
2′,2″-H C_5	2.39, 2.03	2.30, 2.00	2.20, 1.80	2.38, 2.38	2.32, 2.32	2.31, 1.80	2.11, 1.88	2.28, 1.95	2.35, 1.95
2′,2″-H G_6	2.64, 2.39	2.83, 2.55	2.50, 2.25	2.85, 2.51	2.81, 2.45	2.56, 2.35	2.70, 2.40	2.61, 2.38	2.65, 2.40
Imino protons									
C_1:G_6	*f*	*f*	*f*	*f*	*f*				
G_2:C_5	12.93	12.20	12.80	12.15	12.20				
T_3:A_4	—	—	13.45	13.35	13.40				
T_4:A_3	13.55	13.72	—	—	—				

[a] The values of 3′-H, 4′-H and 5′,5″-H of the ribose units are not reported. 2′-H and 2″-H stand for lowfield and upfield proton respectively. [b] For the sake of clarity, the nucleotide units are numbered only for one strand. [c] 25 °C, H_2O–D_2O (9:1), 600 MHz, estimated accuracy within 0.03 ppm. [d] 45 °C, D_2O, 300 MHz, estimated accuracy within 0.03 ppm. [e] A_3 and T_4 for d(CGATCG)$_2$ sequence, T_3 and A_4 for d(CGTACG)$_2$ sequence. [f] Not detected because of the 'fraying' process.

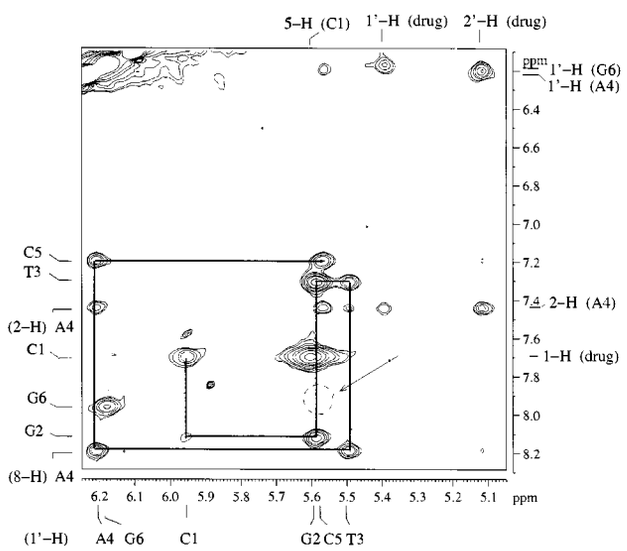

Fig. 3 2D NOESY spectrum of the complex 'TA'–**4** (R = 5.0) in D_2O buffer solution (pH 6.7), 0.1 mol dm^{-3} NaCl at 25 °C, t_{mix} 300 ms, showing the NOE interactions of the ribose 1′-H with the aromatic protons of the bases and with some protons of the drug. The internucleotide NOE connectivities between aromatic and 1′-H protons are traced; for the sake of clarity, the nucleotide units are numbered for only one strand. The arrow indicates the position of the cross peaks 1′-H (C_5)/8-H (G_6) found in the free oligonucleotide, which disappears with intercalation.

and the exchange with the free species, is also reflected in this region of the spectrum. The C_2 symmetry is restored at R values higher than 2. The imino protons were then assigned in the complexes by the NOE interactions which occur between NH protons of neighbouring base-pairs and between NH and the 2-H proton of the adenine in the complementary base. For instance, in the complex of **4** with d(CGATCG)$_2$ the NH of the A_3:T_4 pair shows an NOE interaction with the NH of G_2:C_5 and with the aromatic proton 2-H of A_3. In all the complexes, as a consequence of intercalation, the imino protons connecting the G_2:C_5 base pairs experience an upfield shift of 0.6–0.7 ppm.

The anthraquinone hydrogen-bonded OH protons of the drug become protected from the solvent exchange, as a consequence of intercalation, and resonate in the low-field region of the spectrum together with the imino protons (see Table 4). The 6-OH signal was identified at δ 12.40–12.50 by intramolecular NOE interactions with 1′-H of daunosamine and with 7-H of the adjacent ring A; the 11-OH signal was likewise detected at δ 12.00–12.15 by NOE with the protons at C-10. The protons of the anthracycline molecules in the bound state were attributed based on the assignments of the free drugs[19] and by detecting the NOESY-exchange cross peaks. The assignments of 7-H, 14-H and of the hemiacetalic 2″-H on the morpholino ring, which resonate in a very crowded region of the spectrum, were confirmed by heteronuclear one-bond ^{13}C/^{1}H shift correlation experiments (Table 4). The morpholino protons gave broad signals as a consequence of the conformational mobility of the ring, which still holds in the complexes.

From all these structural data it follows that no covalent complex is formed.

NOE results and structure derivation

When all the protons of the complexes were attributed, many intermolecular interactions could be identified in the 2D NOESY spectrum. The measured NOEs, reported in Table 5, can be grouped as (*i*) intermolecular NOEs at the intercalation site (CG base pairs), and (*ii*) intermolecular NOEs in the minor groove (AT base pairs). (*i*) The position of the anthracycline aglycone was defined by many NOE cross peaks involving the protons at C-4, the hydroxy groups of the anthraquinone ring B and the protons of ring A. Specifically 4-OMe (or 4-H in the case of idarubicin **3**) interacts with the ribose and the aromatic protons of cytidine C_{11}; moreover 11-OH shows contacts with 6-H and 5-H of cytidine C_1, while 6-OH interacts with 8-H of

Table 4 ^{1}H Chemical shift assignments (δ) for the anthracyclines **1**, **2**, **3**, **4** and **5** in the complexes with d(CGTACG)$_2$ and d(CGATCG)$_2$

Anthracycline protons	'TA' + **1**[a]	'TA' + **2**[a]	'TA' + **3**[a]	'TA' + **4**[b]	'TA' + **5**[b]	'AT' + **4**[b]
1-H	7.45	7.53	7.60	7.70	7.70	7.60
2-H	7.51	7.60	7.93	7.70	7.70	7.70
3-H	7.11	7.25	7.35	7.41	7.41	7.38
4-OMe	3.75	3.75	7.70[c]	3.85	3.90	3.80
7-H	4.50	4.85	4.71	4.67	4.52	4.60
8-H_{eq}	2.45	2.55	2.40	2.10	2.40	2.30
8-H_{ax}	2.22	2.35	2.25	1.80	1.96	1.80
10-H_{eq}	2.90	3.01	2.92	3.05	3.00	2.85
10-H_{ax}	2.60	3.01	2.92	2.85	2.80	2.70
6-OH	—	—	—	12.50	12.42	12.40
11-OH	—	—	—	12.15	12.05	12.00
14-H	3.40	2.38	2.45	3.30	3.45	3.35
Daunosamine						
1′-H	5.21	5.50	5.35	5.40	5.41	5.40
2′-H	2.20	2.15	2.10	2.10	2.40	2.10
2″-H	2.20	1.95	1.90	1.90	1.80	1.80
3′-H	3.96	3.94	3.85	3.85	3.82	3.81
4′-H	3.40	3.70	3.56	3.70	3.45	3.85
5′-H	4.25	4.34	4.36	4.31	4.52	4.26
5′-Me	1.15	1.26	1.25	1.35	1.35	1.30
Morpholinyl						
3″-OMe	—	—	—	3.51	—	3.45
2″-H	—	—	—	5.10	—	5.00
–CH_2–	—	—	—	*d*	*d*	*d*

[a] Acquired at 300 MHz in D_2O, 45 °C, t_{mix} 100 ms, estimated accuracy within 0.03 ppm. [b] Acquired at 600 MHz in H_2O–D_2O (9:1), 25 °C, t_{mix} 100 ms. Estimated accuracy within 0.03 ppm. [c] 4-H signal. [d] Not resolved around δ 3.1 and 3.6.

guanine G_{12} on the complementary strand. This indicates that the aglycone moiety is oriented in an orthogonal position with respect to the base pairs C_1:G_{12} and G_2:C_{11}, with ring D protruding out on the major groove. Consequently, ring A of the aglycone must be placed in front of the guanines G_2 and G_{12}, which is confirmed by the NOE interactions involving 10-H_{eq} and 7-H of ring A with the ribose protons 1′-H of G_2 and G_{12} respectively. (*ii*) The orientation of the amino sugar, linked to C-7 of ring A, follows from this result and is further confirmed, in the case of 'TA' complexes, by the NOE contacts involving 1′-H and 5′-Me of daunosamine and ribose protons of guanine G_{12} and timine T_3, respectively. The same interactions were found in the 'AT' complex, where the 1′-H proton of adenine A_3 was in this case involved. These results allow definition of the position of the aminosugar in the minor groove. The morpholino ring of anthracyclines **4** and **5** was defined by the contacts between the hemiacetalic 2″-H proton and 2″-OMe with ribose protons of the fourth unit, T_4 and A_4 for 'AT' and 'TA' complex respectively.

The observed drug–DNA interactions listed in Table 5 were used to build some structural models by restrained molecular mechanics and dynamics calculations (see Experimental section). First we built models by interactive computer graphics by placing the anthracyclines into the double helix, generated as a B-type DNA, in an orientation that qualitatively satisfies the experimentally determined NOE values. Then, all structures were energy-minimized and subjected to a restrained molecular dynamics calculation. No other restraints, except for the interatomic distances obtained by the NOE values and the hydrogen bonds between the DNA base-pairs, were applied. In this way the double helix was allowed to move freely. Table 6 lists the backbone torsion angles derived from the final structure of 'TA' and 'AT' complexes with methoxymorpholinodoxorubicin **4**. An overview of the values of the phosphodiester α and ζ torsion angles shows that most residues are in *gauche*,*gauche* (*g*,*g*) conformation, with two exceptions at the level of C_5pG_6, G_2pA_3 (or G_2pT_3), which are in *gauche*,*trans* (*g*,*t*) conformation for both complexes. This conformational change is coupled with the downfield shift of the corresponding phosphate resonances, as reported in Table 1. However, an inspection of Table 1 shows that the downfield effects are rather different, ranging from 1.12 to 1.57 ppm for C_5pG_6 and from 0.84 to 1.53 ppm for G_2pT_3 (or G_2pA_3). In contrast, the X-ray results on the same

Table 5 Intermolecular NOE interactions between anthracyclines **1**–**5** and oligomer protons in the complexes with d(CGATCG)$_2$ and d(CGTACG)$_2$

Anthracycline proton	'AT' + **4**[a]	'TA' + anthracycline[b]
1-H	5-H (C_1)	5-H (C_1)
3-H	5-H (C_{11})	5-H (C_{11})
4-OMe[d]	2′,2″-H (C_{11})	2′,2″-H (C_{11})[c]
	6-H	6-H
		1′-H[e]
		5-H[e]
6-OH[f]	—	2′,2″-H (C_{11})
		8-H (G_{12})
7-H[f]	1′-H (G_{12})	1′-H (G_{12})
	4′-H	4′-H
10_{eq}-H	—	1′-H (G_2)[g]
		1′-H (C_1)[f]
11-OH	1′-H (C_1)	1′-H (C_1)[f]
	2′, 2″-H	2′,2″-H
	5-H	5-H[f]
	6-H	
1′-H[f]	1′-H (G_{12})	1′-H (G_{12})
3′,4′,5′-H	—	1′-H (T_3)[e]
5′-Me[f]	1′-H (A_3)	1′-H (T_3)
		4′-H[h]
2″-OMe	1′-H (T_4)	1′-H (A_4)
		5′,5″-H[g]
2″-H	1′-H (T_4)	1′-H (A_4)
		4′-H[h]
		2-H[h]

[a] Acquired at 600 MHz in H_2O–D_2O (9:1), 25 °C, t_{mix} 100 ms. [b] Acquired at 300 MHz in D_2O, 45 °C, t_{mix} 100 ms for **1**, **2** and **3**. In the case of 'TA'–**4** complex, experimental conditions as in (*a*). [c] Not detected for the complex with **2**. [d] In the case of **3**, the NOE involves 4-H proton. [e] Observed only for 'TA'–**3** complex. [f] Not detected for the complex with **5**. [g] Detected only for the complex with **3** and **4**. [h] Observed only for 'TA'–**4** complex.

Table 6 Glycosyl and backbone torsion angles (°) for d(CGATCG)$_2$ and d(CGTACG)$_2$ complexes with **4** derived by MD calculations[a]

'AT'[b]	χ	α	β	γ	δ	ε	ζ
$C_{1,7}$	235, 201	—	—	57, 60	120, 143	288, 267	209, 289
$G_{2,8}$	229, 268	303, 283	114, 151	57, 50	95, 136	176, 270	271, 167
$A_{3,9}$	212, 214	297, 285	168, 114	57, 53	77, 73	191, 180	293, 276
$T_{4,10}$	219, 237	288, 296	171, 179	67, 63	92, 130	179, 191	279, 278
$C_{5,11}$	255, 248	297, 285	175, 167	60, 56	137, 119	196, 279	241, 142
$G_{6,12}$	256, 250	297, 280	185, 148	66, 54	147, 142	—	—
'TA'[b]							
$C_{1,7}$	242, 202	—	—	57, 56	69, 137	46, 262	65, 285
$G_{2,8}$	246, 263	248, 284	178, 154	64, 56	143, 138	180, 288	251, 87
$T_{3,9}$	237, 215	293, 120	179, 179	60, 106	123, 80	187, 180	273, 275
$A_{4,10}$	247, 244	283, 292	172, 182	55, 57	113, 137	179, 185	270, 276
$C_{5,11}$	258, 247	296, 287	171, 171	57, 55	128, 113	294, 285	113, 184
$G_{6,12}$	226, 225	120, 225	285, 121	106, 54	75, 80	—	—

[a] Values obtained from the final structure. Probable error estimated within ±12° (see Experimental section). [b] The glycosyl angle χ is O(4′)–C(1′)–N(1)–C(2) and O(4′)–C(1′)–N(9)–C(4) for pyrimidines and purines respectively; the backbone torsional angles are defined as follows: C5′–γ–C4′–δ–C3′–ε–O3′–ζ–P–α–O5′–β–C5′.

units of the two complexes show very similar values for all ζ angles (160–190°), as well as for all α angles (285–310°).[10c,11b] What does the modulation of the ^{31}P chemical shift mean? This apparent discrepancy is caused by the assumption that one single conformer is present in solution. In fact the observed ^{31}P chemical shift is a weighted average of the chemical shifts of the different conformations. In order to have an insight into this conformational equilibrium, we performed more detailed MD calculations. Fig. 4 displays the results obtained after an MD run performed on the 'AT'–**4** complex at 600 K. Every 2 ps a conformation was sampled and the α and ζ torsion angles relative to each phosphate were measured and plotted as a graph. In this way it was possible to recognize the most populated conformations. For example, T_4pC_5 unit is almost completely in the g^-,g^- conformation, corresponding to dihedral angles α (C_5) and ζ (T_4) of −90°. The same occurs for the A_3pT_4 unit, where ζ (A_3) are −90° and α (T_4) values are concentrated around the g^- conformations. The other three units show scattered values. G_2pA_3 and C_5pG_6 display a broad distribution of α and ζ angles in g^-,g^+ and t regions, but the *trans* conformation is significantly more stable for ζ (C_5) and is slightly preferred for α (G_6). In the case of C_1pG_2, the ζ (C_1) angle is entirely in the g^- conformation, while α (G_2) shows values distributed around the g^- and t region. In summary, C_5pG_6 and also G_2pA_3 display a relevant population of *trans* conformers in agreement with the significant down field shift (1–1.6 ppm) observed for the corresponding phosphates, as theoretically predicted.[17] The small down field value (0.5 ppm), always observed for the terminal phosphate C_1pG_2 and interpreted as being caused by the asymmetric shape of the anthracycline which induces a minor deformation on this segment, must be viewed as a consequence of a slight increase in *trans* population for angle α of G_2, rather than for angle ζ of C_1 residue. The other units exist entirely in *gauche* conformations, with a consequent slight or zero change in chemical shift. Therefore the modulation of the ^{31}P chemical shift, as shown by the data in Table 1, can easily be interpreted as changes in conformer populations.

The dynamic variation of the backbone torsional angle ζ is also reflected in a change of the adjacent angle ε, C(4′)–C(3′)–O(3′)–P. A correlation has been found[17b] between angles ζ and ε ($\zeta = -348 - 1.42\ \varepsilon$), based upon a number of B-DNA crystal structures, which have shown that two conformational states are usually observed in B-DNA, named B_I and B_{II}. They are characterized by values $\varepsilon - \zeta$ of *ca.* −90 and +90° respectively. The B_I state has been estimated to be more stable (4.18 kJ mol^{-1}) than the B_{II} conformation and corresponds to $\varepsilon = 170°$ and angle ζ in *gauche* (g^-) conformation, whereas the B_{II} state corresponds to $\varepsilon = 255°$ and angle ζ in *trans* conformation. The ^{31}P chemical shift difference between B_I and B_{II} states has been estimated to be *ca.* 1.6 ppm.[17] The ε values obtained by NMR restrained MD calculation for $G_{2,8}$ and $C_{5,11}$ units are 176 and 196° respectively for one strand of the 'AT'–**4** complex, and 270 and 279° for the other strand (Table 6). The same occurs for the $G_{2,8}$ unit of the 'TA'–**4** complex, whereas for the $C_{5,11}$ unit the ε values are similar (294, 285°) in both strands. This confirms a significant population of the B_{II} state for the above units. In contrast, the internal units A and T show ε values in the range 179–191° corresponding to a pure B_I conformational state.

The backbone torsion angles β do not show a significant variation with respect to the canonical B-DNA and to the Dickerson dodecamer,[20] except for the lower values (114°) obtained for residues G_2 and A_9 in the 'AT'–**4** complex. It is interesting to note that distorsions at the level of the third units for angles β and at the level of $G_{2,8}$ and $C_{5,11}$ for ε angles have also been observed in some crystal structures.[10a,b,11] Therefore these distorsions appear to be correlated with the intercalation of the two anthracycline molecules.

Torsion angles δ, C(5′)–C(4′)–C(3′)–O(3′), exocyclic with respect to the ribose rings, are a measure of the ring puckering and are correlated with the glycosidic angles χ (anticorrelation principle)[20] which are defined as O(4′)–C(1′)–N(1)–C(2) and O(4′)–C(1′)–N(9)–C(4) for pyrimidines and purines respectively. An inspection of Table 6 shows that most of the δ angles display values between 120–150°, coupled with glycosidic angles χ of 230–270°, in agreement with the anticorrelation principle, which predicts values in the range 240–270°, *i.e. anti* (*-ac*) orientation of the bases. This corresponds to C-2′-*endo*–C-1′-*exo* ribose conformations. A deviation from the B-DNA geometry appears at the level of the third nucleotide units: the lowest values (73–80°) of δ angles were found for $A_{3,9}$ and T_9, coupled with χ angles of 210–215° in agreement with the anticorrelation principle. This is in line with the values reported for the solid state (δ 105 and 79° and χ 227 and 215°)[11b] and should correspond to a ribose conformation between O-4′ *endo* and C-3′ *endo*. The terminal G_6, G_{12} and C_1 units also show low values, but they were not considered because of the end effect. The morpholino rings of both intercalated anthracycline molecules display a conformational equilibrium between chair and boat forms, as appears from the variation of the N3′–C5″–C6″–O1″ torsion angle during the 90 ps dynamics simulation. In the energy minimized structure, the two morpholino rings result in opposite chair conformations. This internal motion explains the larger line width observed for all protons on the heterocyclic ring, compared with the other resonances.

Conclusions

The structures derived from NOE and restrained molecular

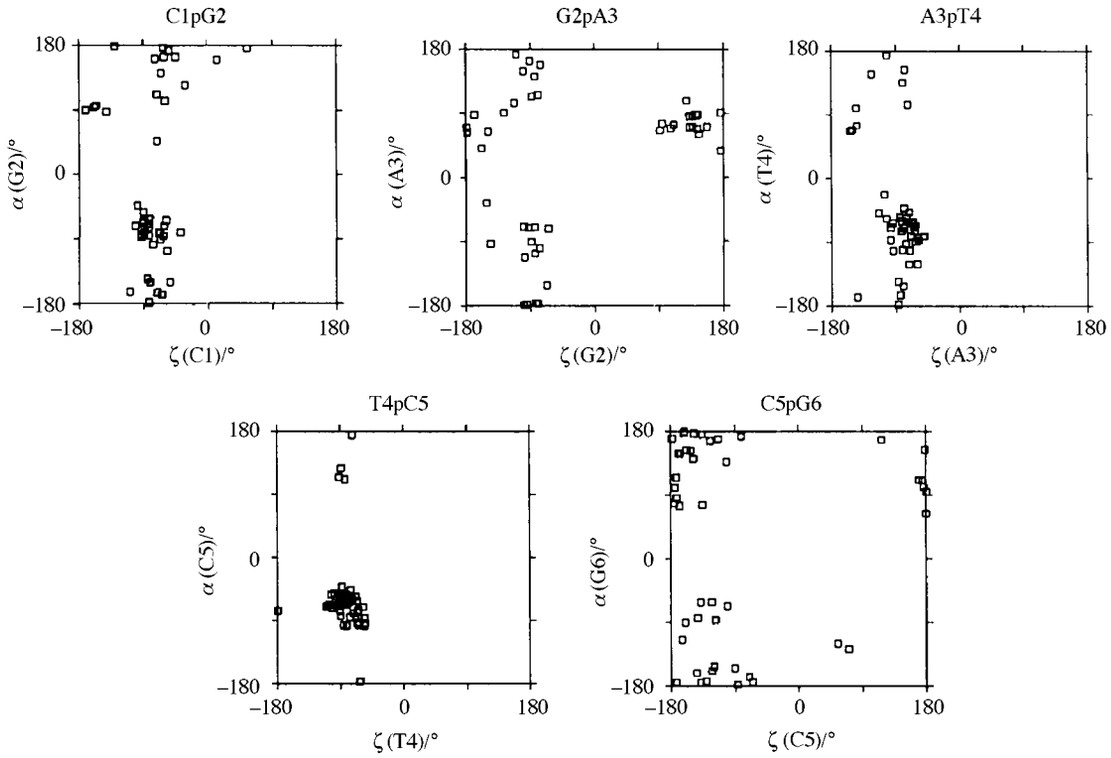

Fig. 4 Correlation between torsion angles α and ζ for the phosphate groups in the 'AT'–**4** complex obtained from 2 ps MD run

dynamics data show the aglycone intercalated and orthogonally oriented between the terminal CG base pairs and located in a central position with respect to the two strands, as appears from the NOE interactions of the aromatic protons 1-H and 3-H of ring D with 5-H of cytidines C_1 and C_{11} respectively. Additional evidence comes from the interactions of the hydroxy protons 11-OH with cytidine C_1 and 6-OH with guanine G_{12} on the complementary strand. The energy minimized structure of the complex 'AT'–**4** is reported in Fig. 5. Ring D extends out of the double helix on the major groove, while ring A lies between guanines G_2 and G_{12}, as proved by NOEs involving 10-H_{eq}, 7-H and the ribose protons of these units. The 4-OMe group on ring D apparently does not affect the intercalation (**3** and **2** have similar k_{off}),[9b] even though it shows contacts (3–3.5 Å) with the ribose protons at C-2′ of C_{11}. Idarubicin **3**, where 4-OMe is replaced by a proton gave similar results, 4-H proton having one NOE contact with 1′-H of the same cytidine.

The distances of 9-O from 3-N (2.9 ± 0.2 Å) and 2-N (3.2 ± 0.3 Å) of G_2 show the possibility of hydrogen bonding involving the hydroxy group at C-9 and guanine G_2, in line with X-ray results.[10,11] Also the distance (3.2 ± 0.2 Å) between 7-O and 2-N (G_2) is the same (3.17 Å) as in the solid phase,[10a] but the conformation of ring A is the half chair $^9H_8$, as in the free doxorubicin,[19] and not the skew ^9S as found in the crystal structure.[10a]

The torsion angles around the glycosyl linkage, C(7)–O(7)–C(1′)–C(2′) and C(20)–C(7)–O(7)–C(1′) are 132 and −167° respectively in 'AT'–**4** complex, values which slightly differ from X-ray results.[11] The daunosamine ring lies in the center of the minor groove for all the complexes, as is shown by the NOE interactions with 1′-H ribose protons of residues A_3 (T_3) and G_{12}, located on opposite strands. Small differences from the X-ray structure thus result,[11a] where the daunosamine ring in the 'TA'–**4** complex is rather close to $G_{2,8}$ units. In the other X-ray study,[11b] this point has not been discussed in detail. On the other hand, in an early X-ray paper on the daunomycin–'TA' complex,[10a] distances have been reported between 2-O of T_3 and daunosamine atoms C-4′ and 3′-N, which are consistent with our results. It must be noted however that in the X-ray

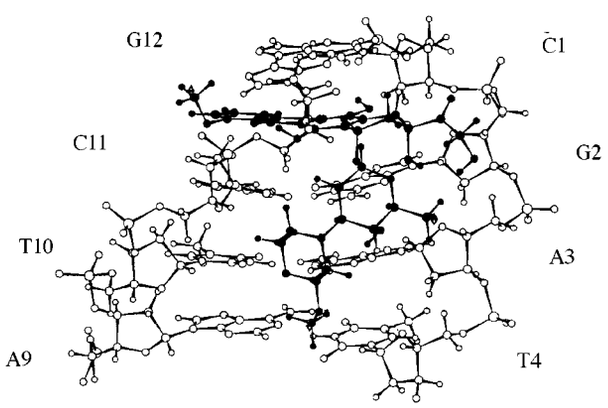

Fig. 5 Energy minimized molecular model of the 'AT'–**4** complex

studies[10b,c] of 'AT'–**1** and 'AT'–**2** complexes the amino sugar has been placed closer to residue C_{11} and T_{10}.

The morpholino ring of the anthracyclines **4** and **5** lies also in the minor groove as defined by NOE contacts involving the hemiacetalic 2″-H proton, 2″-OMe and the ribose protons of the fourth unit (T_4 or A_4). The distance between the two oxygen atoms 1″-O of the morpholino rings was found to be between 3 and 5 Å, owing to the internal mobility of the two rings. This differs from X-ray results,[11] where these atoms are in van der Waals contact, and from a solution structure,[12a] where a distance of 2.3 Å is reported. An inspection of the solvent accessible surface generated from the final structure of the complexes with **4** led to the identification of a cavity between the morpholino 2″-OMe group and the ribose 4′-O atom of T_4 (or A_4) unit. This cavity, in spite of the mobility of the morpholino ring, allows the accommodation of a residual water molecule from the original spine of hydration in the minor groove, which might be involved in hydrogen bonding with OMe and with the ribose 4′-O. Although not proved experimentally, the presence of such water-mediated hydrogen bonds might provide a possible explanation for the lower value of the k_{off} observed for **4** *vs.* **5**. The higher cytotoxicity of **4** with respect to **5**[3b] is also in

agreement with the longer residence time of **4**. The strong decrease of k_{off} found for both complexes of **4**, with respect to the parent compound **1**, is in line with the activity *in vitro* and *in vivo*, and shows that the variation in the nucleotide sequence does not affect the k_{off} of **4**. On the contrary, in the case of doxorubicin **1** the 5′-CGT sequence seems to be slightly more favoured than the 5′-CGA (k_{off} 17.3 *vs.* 23.0 s^{-1}). This latter result is in contrast with the conclusions drawn from X-ray structures, where the hydrogen bonds involving 3′-N of daunosamine should stabilize the 'AT', but not the 'TA' complex.

The intercalation of these large molecules induces conformational changes in the phosphoribose backbone, which are revealed by both ^{1}H and ^{31}P NMR data. The sequence of the characteristic NOE interactions breaks off at the level of CG residue, *i.e.* the NOE contact between ribose 1′-H of $C_{5,11}$ and 8-H of $G_{6,12}$ is no longer occurring, as the distance between them is now greater than 5 Å. On the other strand the intensity of the NOE cross peaks connecting 8-H of $G_{2,8}$ with 1′-H of $C_{1,7}$ is significantly weak. Thus $C_{5,11}$ and $G_{6,12}$ and to a lesser extent $C_{1,7}$ and $G_{2,8}$ are more displaced from each other, in order to accommodate the intercalating molecules. The upfield shift of 0.6–0.7 ppm observed for the G_2:C_5 imino protons in all the complexes must be due to the ring current shift exerted by the anthraquinone moiety, rather than to a lengthening of the hydrogen bonds connecting the complementary bases at the intercalation site.

The deformations of the phosphoribose backbone are coupled with a down field shift of the corresponding phosphates, which in our complexes ranges from 0.5 to 1.6 ppm. The largest effects were observed for phosphates C_5pG_6 (1.12–1.57 ppm) and G_2pT_3 or G_2pA_3 (0.84–1.53 ppm), but the former is in general the most deshielded, providing further evidence of the intercalation sites between the terminal CG pairs. In the solid state structures,[10,11] the α and ζ torsional angles around the P–O bond are all in the *gauche* conformation, except for the above residues which are in α-*gauche* and ζ-*trans* conformations. The modulation of the observed ^{31}P chemical shift values suggests that a conformational equilibrium occurs among differently populated conformers. The MD calculations showed that C_5pG_6 and G_2pT_3 (G_2pA_3) indeed display a relevant population of *trans* conformers for ζ and also α angles. By contrast, the initial phosphate C_1pG_2 displays a small down field shift (0.5 ppm), corresponding to a slight increase in the *trans* population for angle α of G_2. All the other units exist entirely in α, ζ *gauche*,*gauche* conformation in agreement with constant chemical shifts. The dynamic variations of the two correlated angles ζ and ε at the level of $G_{2,8}$ and $C_{5,11}$ residues in both complexes with **4** confirm a significant population of the less stable[17b] B_{II} state at the intercalation sites. A deviation from the B-DNA geometry also appears at the level of the third residue, for angle δ and for the correlated glycosyl angle χ. The low values of δ for $A_{3,9}$ and T_9 are in line with those found in the solid state and should correspond to ribose conformations between O-4′ *endo* and C-3′ *endo*. The β torsion angles are more constant, however small deformations for residues G_2 and A_9 were observed in 'AT'–**4** complex, which appear to be related with the intercalation.

Acknowledgements

We are indebted to MURST for financial support and to Pharmacia & Upjohn for the kind gift of anthracyclines.

References

1 (*a*) F. Arcamone, *Doxorubicin: Anticancer Antibiotics*, New York, Academic Press, 1981; (*b*) S. Penco and F. Arcamone, *Molecular aspects of anticancer drug action*, ed. J. W. Lown, Macmillan Press, London, 1988; (*c*) R. D. Anderson, M. L. Veigl, J. Baxter and W. D. Sedwick, *Cancer Res.*, 1991, **51**, 3930.
2 (*a*) E. M. Acton, G. L. Tong, C. W. Mosher and R. L. Wolgemuth, *J. Med. Chem.*, 1984, **27**, 638; (*b*) A. Bargiotti, P. Zini, S. Penco and F. Giuliani, *US Pat.*, 4 672 057, 1987; (*c*) N. Komeshima, H. Kawai, S. Nakajima, M. Watanabe, T. Tsurno, T. Takeuchi and N. Otake, *J. Antibiot.*, 1989, **42**, 1425.
3 (*a*) J. Westendorf, M. Aydin, G. Groth, O. Weller and H. Marquardt, *Cancer Res.*, 1989, **49**, 5262; (*b*) M. Grandi, G. Pezzoni, D. Ballinari, L. Capolongo, A. Suarato, A. Bargiotti, D. Faiardi and F. Spreafico, *Cancer Treat. Rev.*, 1990, **17**, 133; (*c*) P. A. Vasey, D. Bisset, M. Strolin-Benedetti, I. Poggesi, M. Breda, L. Adams, P. Wilson, M. A. Pacciarini, S. B. Kaye and J. Cassidy, *Cancer Res.*, 1995, **55**, 2090.
4 (*a*) S. Neidle and M. Waring, *Molecular Aspects of Anticancer Drug-DNA Interactions*, Macmillan Press, London, 1993; (*b*) W. B. Pratt, R. W. Ruddon, W. D. Ensminger and J. Maybaum, *The Anticancer Drugs*, Oxford University Press, London, 1994; (*c*) G. Capranico, E. Butelli and F. Zunino, *Cancer Res.*, 1995, **55**, 312.
5 (*a*) C. Cullinane, S. M. Cutts, A. van Rosmalen and D. R. Phillips, *Nucleic Acids Res.*, 1994, **22**, 2296; (*b*) C. Cullinane and D. R. Phillips, *Biochemistry*, 1994, **33**, 6207.
6 F. Leng, R. Savkur, I. Fokt, T. Przewloka, W. Priebe and J. B. Chaires, *J. Am. Chem. Soc.*, 1996, **118**, 4731.
7 B. Pullman, *Anti-Cancer Drug Des.*, 1991, **7**, 95.
8 (*a*) J. M. Neumann, J. A. Cavailles, M. Herve, S. Tran-Dinh, B. Langlois d′Estaintot, T. Huynh-Dinh and J. Igolen, *FEBS Lett.*, 1985, **182**, 360; (*b*) J. B. Chaires, K. R. Fox, J. E. Herrera, M. Britt and M. J. Waring, *Biochemistry*, 1987, **26**, 8227; (*c*) V. Rizzo, C. Battistini, A. Vigevani, N. Sacchi, G. Rozzano, F. Arcamone, A. Garbesi, F. P. Colonna, M. Capobianco and L. Tondelli, *J. Mol. Recognit.*, 1989, **2**, 132.
9 (*a*) E. Ragg, R. Mondelli, C. Battistini, A. Garbesi and F. P. Colonna, *FEBS Lett.*, 1988, **236**, 231; (*b*) R. Bortolini, S. Mazzini, R. Mondelli, E. Ragg, C. Ulbricht, S. Vioglio and S. Penco, *Appl. Magn. Reson.*, 1994, **7**, 71.
10 (*a*) A. H. J. Wang, G. Ughetto, G. J. Quigley and A. Rich, *Biochemistry*, 1987, **26**, 1152; (*b*) M. H. Moore, W. N. Hunter, B. Langlois d′Estaintot and O. Kennard, *J. Mol. Biol.*, 1989, **206**, 693; (*c*) A. Frederick, L. D. Williams, G. Ughetto, G. A. van der Marel, J. H. van Boom, A. Rich and A. H. J. Wang, *Biochemistry*, 1990, **29**, 2538; (*d*) Y. G. Gao and A. H. J. Wang, *Anti-Cancer Drug Des.*, 1991, **6**, 137.
11 (*a*) M. Cirilli, F. Bachechi, G. Ughetto, F. P. Colonna and M. L. Capobianco, *J. Mol. Biol.*, 1992, **230**, 878; (*b*) Y. G. Gao and A. H. J. Wang, *J. Biomol. Struct. Dyn.*, 1995, **13**, 103.
12 (*a*) C. Odefey, J. Westendorf, T. Dieckmann and H. Oschkinat, *Chem. Biol. Interact.*, 1992, **85**, 117; (*b*) J. Igarashi and M. Sunagawa, *Bioorg. Med. Chem. Lett.*, 1995, **5**, 2923.
13 H. Chen and D. J. Patel, *J. Am. Chem. Soc.*, 1995, **117**, 5901.
14 (*a*) L. Braunschweiler and R. R. Ernst, *J. Magn. Reson.*, 1983, **53**, 521; (*b*) A. Bax and D. G. Davis, *J. Magn. Reson.*, 1985, **65**, 355; (*c*) V. Sklenàr and A. Bax, *J. Magn. Reson.*, 1987, **74**, 469; (*d*) A. Bax, R. H. Griffey and B. L. Hawkins, *J. Magn. Reson.*, 1983, **55**, 301; (*e*) M. R. Bendall, D. T. Pegg and D. M. Doddrell, *J. Magn. Reson.*, 1983, **52**, 81.
15 S. J. Weiner, P. A. Kollman, D. A. Case, U. C. Singh, C. Ghio, G. Alagona, S. Jr. Profeta and P. Weiner, *J. Am. Chem. Soc.*, 1984, **106**, 756.
16 (*a*) J. W. Lown, C. C. Hanstock, R. C. Bleackley, J. L. Imbach, B. Rayner and J. J. Vasseur, *Nucleic Acids Res.*, 1984, **12**, 2519; (*b*) L. Nilsson, G. M. Clore, A. M. Gronenborn, A. T. Brünger and M. Karplus, *J. Mol. Biol.*, 1986, **188**, 455; (*c*) M. Delepierre, T. Huynh Dihn and B. P. Proques, *Biopolymers*, 1989, **28**, 2115.
17 (*a*) D. G. Gorenstein, *Phosphorus-31 NMR. Principles and Applications*, Academic Press, New York, 1984; (*b*) D. G. Gorenstein, *Chem. Rev.*, 1994, **94**, 1315 and references cited therein.
18 K. Wutrich, *NMR of Proteins and Nucleic Acids*, Wiley, New York, 1986.
19 (*a*) R. Mondelli, E. Ragg, G. Fronza and A. Arnone, *J. Chem. Soc., Perkin Trans. 2*, 1987, 15; (*b*) R. Mondelli, E. Ragg and G. Fronza, *J. Chem. Soc., Perkin Trans. 2*, 1987, 27.
20 W. Saenger, *Principles of Nucleic Acid Structure*, Springer-Verlag, New York, 1984 and references cited therein.

Paper 8/02350F
Received 25*th March* 1998
Accepted 24*th June* 1998